THORIUM RECOVERY FROM THE TUNGSTEN WELDING ELECTRODES BY ELECTROLYSIS AND NANOFILTRATION

Geani Teodor MAN[1,2], Paul Constantin ALBU[3], Diana Ionela POPESCU (STEGĂRUȘ)[2,*], Violeta-Carolina NICULESCU[2], Virgil Emanuel MARINESCU[4], Aurelia Cristina NECHIFOR[5]

Waste from devices, electrical and electronic equipment (EEED) contains metal elements that are recyclable both for their value and because, if they are not recovered, they can affect the environment. A special case of EEED is represented by tungsten electrodes used for welding at high temperatures. They contain tungsten, which must be recovered for its technical-economic value, and thorium, a radioactive element. The advanced recovery of thorium must be done because even in small quantities it is toxic, being a heavy metal, but also because due to its radioactivity. This paper presents the recovery of thorium from tungsten electrodes by electrolysis and nanofiltration. The choice of the working parameters was made by superimposing the Pourbaix diagrams of the two elements: pH 2 and 12 at an electrochemical potential value of 2.0 V. Under the chosen working conditions, the recovery of thorium is achieved up to the limit of 0.1 ppm.

Keywords: nanofiltration; Pourbaix diagrams; thorium recovery; tungsten electrolysis; tungsten welding.

1. Introduction

The appearance of thorium in EEED wastes is surprising, but also undesirable [1,2]. The presence of thorium in EEED is caused by its multiple domestic applications (crucibles, electric mantles, refractory bricks, opto-

[1] PhD candidate., Dept.of Analytical Cemistry and Environmental Engineering, University National of Science and Technology POLITEHNICA, Bucharest, Romania, e-mail: geani.man@icsi.ro;

[2] PhD., National Research and Development Institute for Cryogenic and Isotopic Technologies—ICSI Rm. Valcea, 4th Uzinei Street, 240050 Ramnicu Valcea, Romania, e-mail: diana.stegarus@icsi.ro (D.I.P.); violeta.niculescu@icsi.ro (V.-C.N.)

[3] Radioisotopes and Radiation Metrology Department (DRMR), IFIN Horia Hulubei, 023465 Măgurele, Romania; e-mail: paul.albu@nipne.ro

[4] PhD., Department of Physico-chemical tests, National Institute for Research and Development in Electrical Engineering ICPE-CA Bucharest, Romania, e-mail virgil.marinescu@icpe-ca.ro

[5] Prof., Dept.of Analytical Cemistry and Environmental Engineering, University National of Science and Technology POLITEHNICA, Bucharest, Romania, e-mail: cristina.nechifor@upb.ro

electronic devices) [3,4]. Thorium is also used to make welding electrodes for high temperatures [5,6]. The concentration of thorium in tungsten welding electrodes is varying between 1.0 and 7.0%, which requires its recuperative separation [8] In the nanofiltration (NF) of aqueous solutions of thorium, RETENTION (*R)* grows from 94 to 99% with pH increasing from 1 to 3.5. At pH 3–9, the retention of thorium remains constant, and in alkaline solutions (pH > 9), values of *R* decrease. [9]. The hydrometallurgical and extractive processes assume acid or basic digestion of the thorium source followed by recovery, mainly through extraction or ion exchange [10,11], but also through various membrane processes [12-15].

This study highlights the recovery of thorium from tungsten electrodes by electrolysis and nanofiltration. The work was carried out with nanofiltration membranes based on Chitosan/Polypropylene hollow fiber membranes (Chi/PPHFM) and - sulfonated-ethylene-propylene-diene-terpolymer/Poly-propylene hollow fiber membranes (sEPDM/PPHFM)

2. Experimental part

2.1. Materials and reagents

2.1.1. Reagents

All reagents and organic compounds used in the presented work were of analytical grade. $Th(NO_3)_4 \cdot 5H_2O$, KSCN, NaOH pellets, HCl 35% suprapure and NH_4OH 25% (analytical grade) were purchased from Merck KGaA (Darmstadt, Germany).

Aluminon, chitosan and Torin (analytical grade, Sigma-Aldrich Chemie GmbH, Steinheim, Germany) were used within the study.

The purified water characterized by 18.2 μS/cm conductivity was obtained with a RO Millipore system (MilliQ® Direct 8 RO Water Purification System, Merck (Darmstadt, Germany) [16].

2.1.2. Materials

The welding electrodes- red band type were purchased from ProConstruct Distribution SRL (Balotești, Romania).

The hollow fibers polypropylene support membranes (PHF-M) were provided by GOST Ltd. (Perugia, Italy) [17,18].

All polymer materials characteristics are detailed in Table 1 [19,20].

Table 1.

The characteristics of the used polymer compounds

Polymers	Name and Symbol	Molar mass (g/mol)	pKa	Solubility (g/L)
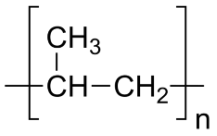	Polypropylene (PP)	cca. 300,000	7.0	-
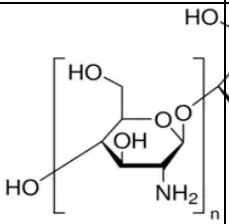	Chitosan (Chi)	5,600	6.2 to 7.0	HCl solution
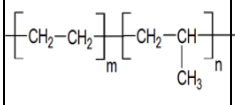	sulfonated ethylene-propylene-diene terpolymer (sEPDM)	3,500-6,000	up to 2.2	organic polar solvents

2.2. Methods and procedures

2.2.1. W-Th anode electrolysis

The electrolysis of W-Th welding electrodes was carried out in a cell with two compartments and three electrodes (Fig. 1). The electrodes were W-Th welding electrode anode, tungsten cathode and reference electrode. The electrolyte was either an acidic solution (HCl) or a basic solution (NaOH) [21]. The potential of the anode was maintained constant 2.0V, imposed by MASTECH HY3005D-3, a power supply which has an electrical output, continuously adjustable, at 0-30V DC and 0-5A.

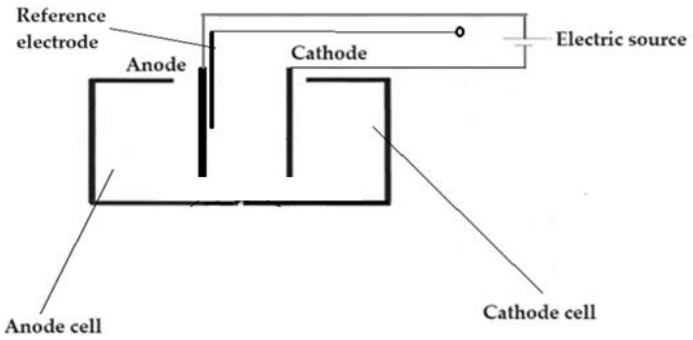

Fig. 1. Electrolysis cell with three electrodes

2.2.2. Preparation of nanofiltration membranes

In this study, two types of polymer/polypropylene hollow fiber membranes were used [22,23] (Fig 2):

- Chitosan/Polypropylene hollow fiber membranes (Chi/PPHFM)
- Sulfonated-ethylene-propylene-diene-terpolymer/Polypropylene hollow fiber membranes (sEPDM/PPHFM)

The membranes were prepared at 6 atmospheres by the nanofiltration of an acidic aqueous solution of 2% chitosan (Fig. 1a) and, respectively, by the nanofiltration of a benzene solution of 2% sEPDM (Fig. 2b). Two types of membranes on a polypropylene support were obtained: Chi/PPHFM and sEPDM/PPHFM, the permeate being the corresponding solvent, and a solution containing traces of chitosan or sEPDM was obtained as a residue.

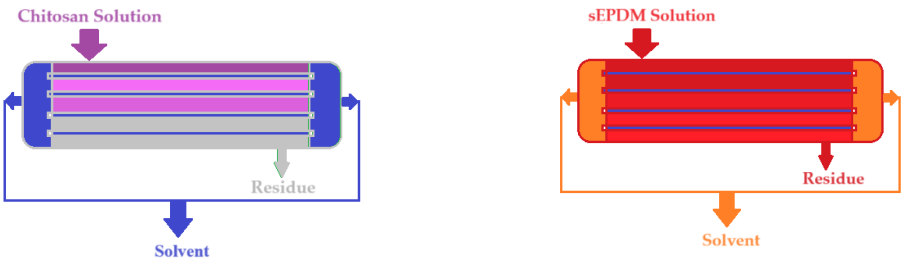

a **b**

Fig. 2. The nanofiltration modules: a) Chi/PPHFM membrane and b) sEPDM/PPHF membrane obtaining.

2.2.3. Nanofiltration of thorium dioxide dispersions

Nanofiltration of thorium dioxide dispersions was carried out, at a pressure of 5-9 atmospheres, through the two types of membranes prepared in a module (Fig. 3):

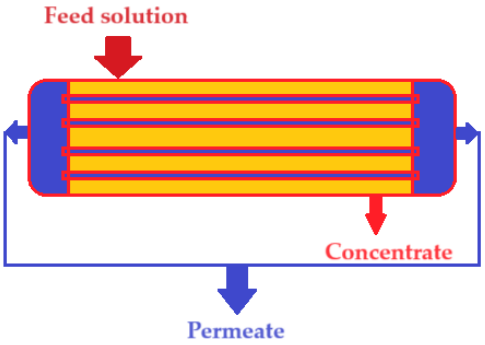

Fig. 3. Nanofiltration of thorium dioxide dispersions in solutions of imposed pH (feed solution)

In Fig. 3 the dispersion was the feed solution, the concentrate contained thorium dioxide, and the permeate was an aqueous solution with an imposed pH. The result of the nanofiltration was presented in the form of the permeate flow (J) (eq.1) and the retention, or of the nanofiltration efficiency (EE) (eq.2):

$$J = \frac{V}{S \cdot \Delta t}\,(L/m^2 h) \tag{1}$$

where: J- permeate flux; V - permeate volume; S-surface of the membrane; Δt - operating interval.

$$EE(\%) = \frac{(c_0 - c_f)}{c_0} \cdot 100 \tag{2}$$

where: EE – separation efficiency (%); C_0 - concentration of nanodispersion (feed solution); C_f - final concentration.

The concentration of the thorium ion was determined by the Torin spectrophotometric method [24]. on a UV-Vis Spectrometer CamSpec M550 device (Spectronic CamSpec Ltd., Leeds, UK).

The tungstate ion concentration was also determined spectrophotometrically with sulfocyanide on a Varian Cary 50 device (Agilent Technologies Inc., Santa Clara, California, US). The specific determinations are caried-out coupled ion-exchange separation and spectrophotometric detection at λ= 405 nm [25].

The obtained results have a precision of 0.1ppm imposed both by the traceability of the samples taken and by the spectrophotometric methods approached.

The morphological and structural characterization of the welding electrodes was carried out with the help of the FESEM-FIB workstation (scanning electron microscope with field emission for electrons and focused ion beam) model Auriga produced by Carl Zeiss SMT Germany through the secondary electron/ion detector (SESI) in the sample room for the topography/morphology

of the surface of the analysed samples [26]. The chemical composition was estimated with the help of the EDS (energy dispersive spectrum for characteristic X-ray) probe produced by Oxford Instruments, UK – model X-MaxN energy dispersive spectrometer with Aztec work and processing software integrated on the FESEM-FIB Auriga workstation [27].

4. Results and discussion

It can be observed that the macroscopic image of the electrode surface (Fig. 4a) is smooth and homogeneous, as is the fracture (section) image (Fig. 4b). The composition of the chosen area (Fig. 4c) was W 93.3 %; O 5.3 % and Th 1.5 % (Fig. 4d).

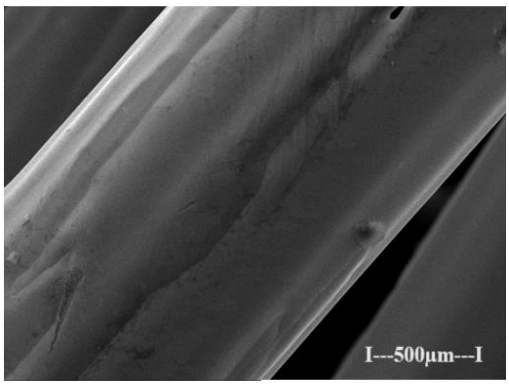

a

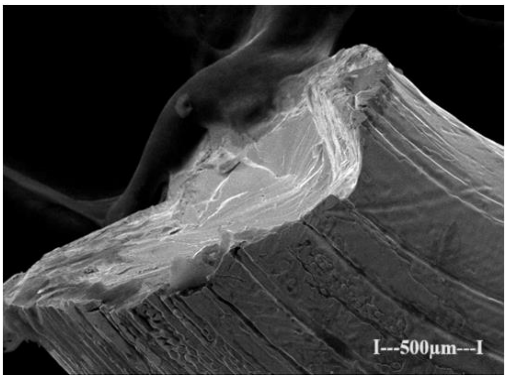

b

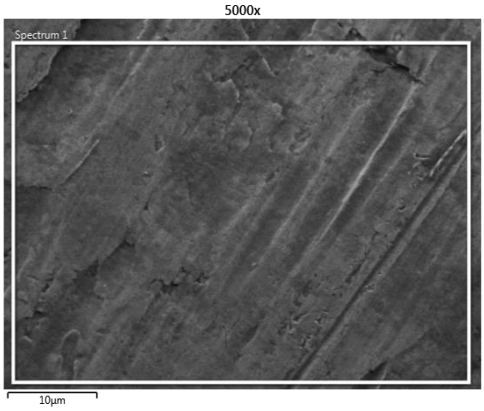

c

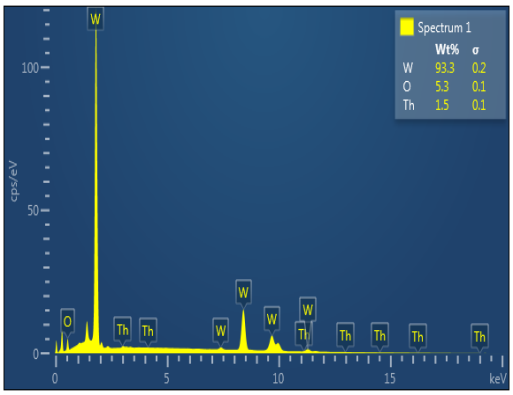

d

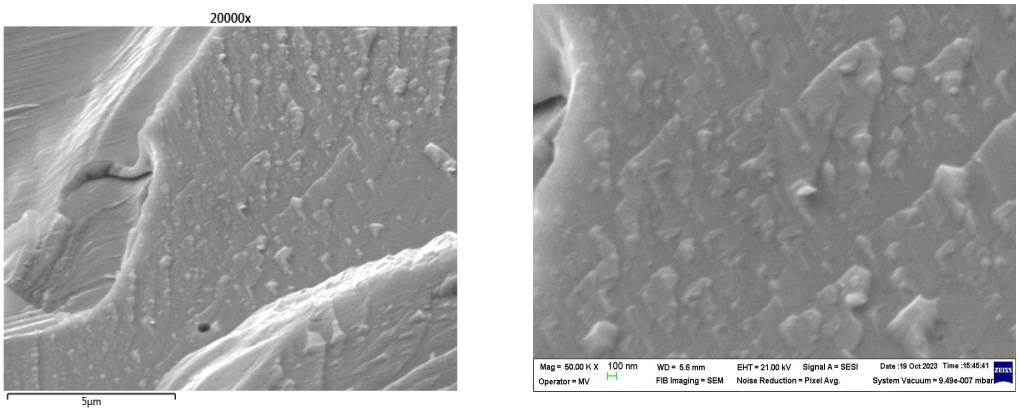

e f

Fig. 4. The morphology of the W-Th welding electrode before electrolysis: a) macrostructure of the electrode surface; b) the image of the fracture of the electrode; c) the area chosen for determining the composition; d) EDX spectrum of the selected area, e) and f) microstructural details

The images from figure 4. (e and f) show the microstructure, respectively the detail of the microstructure of the electrode. These images reveal the tungsten matrix and thorium oxide prisms.

After two hours of electrolysis, the surface of the electrode was analysed (Fig. 5), observing, in the chosen area (Fig. 5b), the removal of thorium from the matrix of the tungsten electrode. In this case, the composition determined by EDAX revealed W 94.3 % and O 5.7 %.

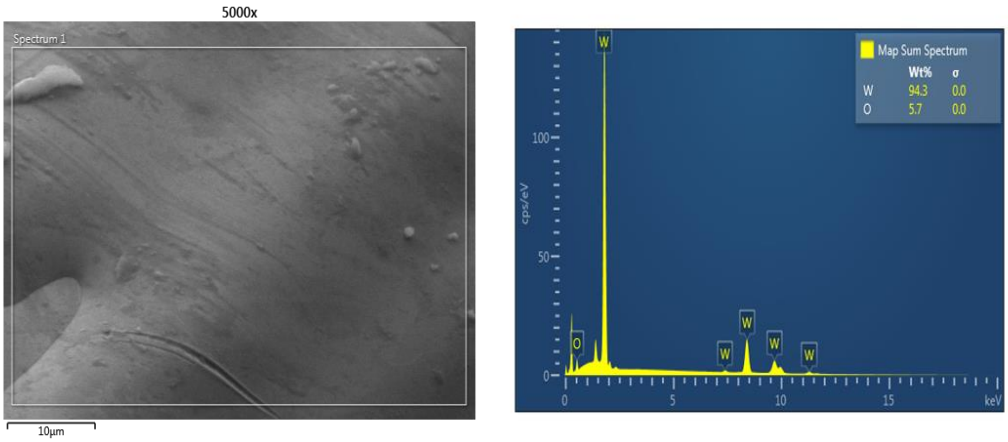

Fig. 5. Microstructure of the electrode area after anodic dissolution of thorium (a) and EDX analysis of the selected area

For the complete dissolution of the welding electrode, the electrolysis continued for 6 hours.

Electrolysis was performed in two variants:

- Acid electrolyte (pH 1)

- Basic electrolyte (pH 13).

The electric potential of the anode was imposed at the value of 2.V, and the choice of the two pH values of the feed solutions of the electrolysis cell was achieved following the interpretation of the Pourbaix diagrams of the two elements tungsten and thorium (Fig. 6) [28-30]:

- at pH 1, the thermodynamically stable chemical species are tungstic acid ($WO_3 \cdot H_2O(s)$) and thorium ion, $Th^{4+}(aq)$.

- at pH 13, the thermodynamically stable chemical species are thorium dioxide ($ThO_2(s)$) and tungstate ion, $WO_4^{2-}(aq)$.

As observed for every electrolysis cases, nanodispersions containing solid nano species were obtained: either tungstic acid or thorium dioxide.

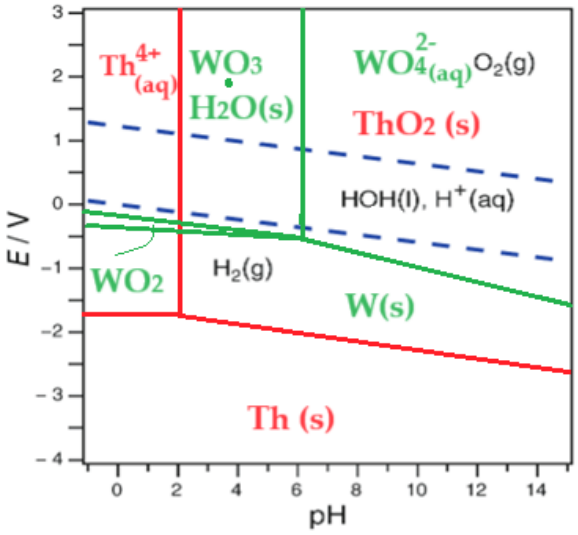

Fig. 6. . Overlaid Pourbaix diagrams of thorium (red) and tungsten (green) and the stability domain of water (blue parallels)

The nanodispersions were nanofiltered through the chitosan nanofiltration membrane (Chi/PPHF) for the acid solution containing tungstic acid ($WO_3 \cdot H_2O(s)$) and thorium ion $Th^{4+}(aq)$, respectively through the sEPDM membrane (sEPDM/PPHFM) for the solution basic containing thorium dioxide ($ThO_2(s)$) and tungstate ion $WO_4^{2-}(aq)$.

The nanofiltration results were presented in the form of flux through the membranes depending on the operating pressure for: pure water, acidic solution containing tungstic acid ($WO_3 \cdot H_2O(s)$) and thorium ion $Th^{4+}(aq)$, and, respectively, the basic solution containing the dioxide of thorium ($ThO_2(s)$) and the tungstate ion $WO_4^{2-}(aq)$ (Fig. 7).

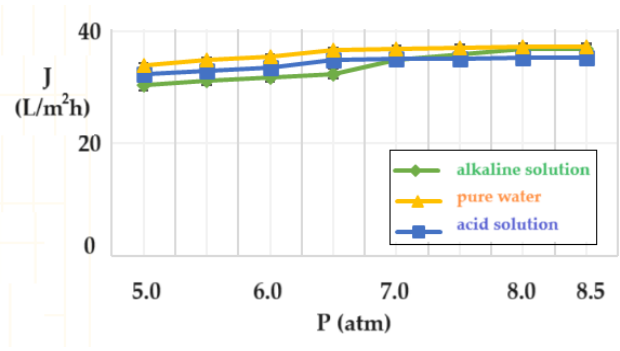

Fig. 7. The variation of the flows (J) of pure water, acid and respectively alkaline nanodispersion as a function of pressure in the nanofiltration module

In all three cases, the permeate flows increased with the increase of the applied pressure. However, the slope of the three curves differed significantly from 5 atmospheres to 7 atmospheres, after which the curves had the same shape, the value differences entering the range of measurement errors (Fig 7).

Separation efficiency (EE) of nanodispersions (Fig. 8) for the acidic solution containing tungstic acid ($WO_3 \cdot H_2O(s)$) and the thorium ion $Th^{4+}(aq)$ and, respectively, the basic solution containing thorium dioxide ($ThO_2(s)$) and tungstate ion $WO_4^{2-}(aq)$ significantly different. Thorium dioxide was retained on the sEPDM membrane (sEPDM/PPHFM) more effectively than the tungstic acid on the chitosan nanofiltration membrane (Chi/PPHF).

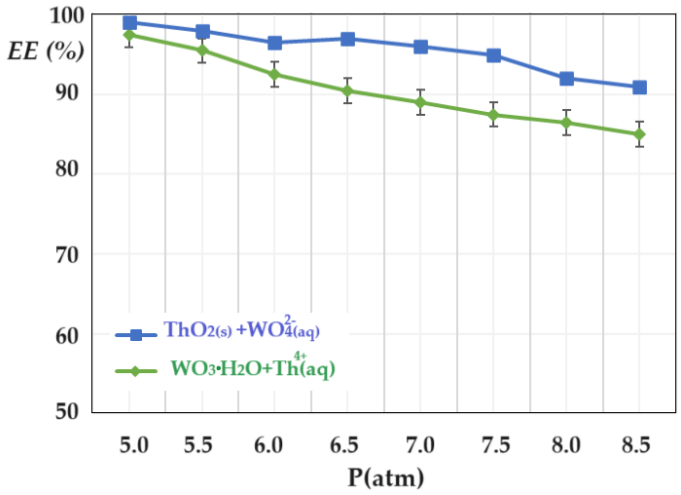

Fig. 8. . The variation of the separation efficiency (EE) of acid and respectively alkaline nanodispersion as a function of pressure in the nanofiltration module

The nanofiltration results can be explained both by the charges of the two membranes: positive for chitosan ($R\text{-}NH_4^+$) and negative for sEPDM ($Ar\text{-}SO_3^-$) [31-33]. As well as by the crystallization form of the dispersed nanoparticles,

tungstic acid and thorium dioxide, respectively. Although the decrease in the separation efficiency (EE) occurs in the working pressure range, all that can be maintained above 85% for both types of nanodisperses and, respectively, membranes (Fig.8). The error bars are significant considering the repeated collection on samples of different parts of the membranes and with nanodispersions with dynamic morphology.

In the case of nanofiltration of the acidic solution, thorium was found in the permeate as Th^{4+} ion, and when filtering the basic solution, thorium was retained on the membrane as thorium dioxide. At the same time, tungsten can be recovered as tungstic acid, which concentrates on the Chi/PPHFM membrane, or as tungstate in the permeate obtained through the sEPDM/PPHFM membrane.

The obtained results are in good correlation with the results presented in the specialized literature [9, 34].

5. Conclusions

Among the waste of electrical and electronic devices and equipment (EEED) those containing thorium are considered extremely dangerous.

In this study, a procedure for efficient separation of thorium from waste welding electrodes at high W-Th temperatures was presented.

For the mineralization of the electrodes, electrolysis was chosen in a strongly acidic (pH 1) or strongly basic (pH 13) environment at an anodic potential of 2.0 V. After electrolysis, thorium separation was achieved by nanofiltration through a Chi/PPHFM membrane for the acid solution and nanofiltration through a sEPDM/PPHFM membrane for the basic solution.

The thorium ion was recovered from the acidic solution within the permeate, while the thorium dioxide was recovered from the basic solution in the concentrate. Simultaneously with the thorium recovery, tungsten was also recovered from the membrane processes as tungstic acid, and respectively, tungstate ion. The thorium separation efficiency (EE) was over 95% at the operating pressure of 5 atm.

R E F E R E N C E S

[1]. *M.G.K. Houessionon, E.-M.D. Ouendo, C. Bouland, S.A. Takyi, N.M. Kedote, B. Fayomi, J.N. Fobil, N. Basu,* Environmental Heavy Metal Contamination from Electronic Waste (E-Waste) Recycling Activities Worldwide: A Systematic Review from 2005 to 2017. Int. J. Environ. Res. Public Health, ***vol.* 18**, 2021, 3517. https://doi.org/10.3390/ijerph18073517

[2]. *G.T. Man, P.C. Albu, A.C. Nechifor, A.R. Grosu, S.-K. Tanczos, V.-A. Grosu, M.-R. Ioan, G. Nechifor,* Thorium Removal, Recovery and Recycling: A Membrane Challenge for Urban Mining. Membranes **vol. 13**, 2023, 765. https://doi.org/10.3390/membranes13090765

[3] *I. Pohjalainen, I.D. Moore, S. Geldhof, V. Rosecker, J. Sterba, T. Schumm, Gas* cell studies of thorium using filament dispensers at IGISOL. Nuclear Instruments and Methods in Physics Research Section B: Beam Interactions with Materials and Atoms **vol. 484**, 2020, pp. 59-70, https://doi.org/10.1016/j.nimb.2020.08.012.

[4]. *T. Ault, S. Krahn, A. Croff,* Comparing the environmental impacts of uranium- and thorium-based fuel cycles with different recycle options. Prog. Nucl. Energy **vol.100,** 2017, pp. 114–134. https://doi.org/10.1016/j.pnucene.2017.05.010

[5]. *E.S. Aziman, A.H.J. Mohd Salehuddin, A.F. Ismail,* Remediation of thorium (IV) from wastewater: Current status and way forward. Separation & Purification Reviews, **vol. 50**, no. 2, 2021**,** pp.177-202. https://doi.org/10.1080/15422119.2019.1639519

[6]. *I.U. Rahman, H.J. Mohammed, M.F. Siddique, M. Ullah, A. Bamasag, T. Alqahtani, S. Algarni,* Application of membrane technology in the treatment of waste liquid containing radioactive materials. Journal of Radioanalytical and Nuclear Chemistry, **vol. 2023**, pp.1-14. https://doi.org/10.1007/s10967-023-09169-9

[7]. *S.V.S.H. Pathapati, M.L. Free, P.K. Sarswat,* A Comparative Study on Recent Developments for Individual Rare Earth Elements Separation. Processes **vol. 11**, 2023, p. 2070. https://doi.org/10.3390/pr11072070

[8]. *H.R. Arabi, S.A. Milani, H. Abolghasemi, F. Zahakifar,* Recovery and transport of thorium (IV) through polymer inclusion membrane with D2EHPA from nitric acid solutions. Journal of Radioanalytical and Nuclear Chemistry, **vol. 327**, 2021. pp.653-665.

[9]. *V.O. Kaptakov, V.V. Milyutin, N.A. Nekrasova, P.G. Zelenin, Kozlitin, E.A.* Nanofiltration Extraction of Uranium and Thorium from Aqueous Solutions. Radiochemistry **vol. 63**, 2021, pp. 169–172. https://doi.org/10.1134/S1066362221020065.

[10]. *P. Ilaiyaraja, A.K.S. Deb, D. Ponraju,* Removal of uranium and thorium from aqueous solution by ultrafiltration (UF) and PAMAM dendrimer assisted ultrafiltration (DAUF). Journal of Radioanalytical and Nuclear Chemistry, **vol. 303**, 2015, pp. 441-450.

[11]. *H. Gomaa, M.Y. Emran, M.M. Elsenety, R.D. Abdel-Rahim, Q. Deng, M.I. Gadallah, M. Saad, H. ALMohiy, M. Ezzeldien, T.A. Seaf El-Nasr, M.S. El-Gaby,* Detection and Selective Removal Strategy of Thorium Ions Using a Novel Fluorescent Ligand and Hybrid Mesoporous γ-Al2O3-like Nanoneedles. ACS Sustainable Chemistry & Engineering **vol. 11**, no. 6, 2023, pp. 2127-2138. https://doi.org/10.1021/acssuschemeng.2c05000

[12]. *M. Tsezos, Volesky*, B. Biosorption of uranium and thorium. Biotechnol. Bioeng. **vol. *23***, 1981, pp. 583–604. https://doi.org/10.1002/bit.260230309

[13]. *D. Hritcu, D. Humelnicu, G. Dodi, M.I. Popa,* Magnetic chitosan composite particles: Evaluation of thorium and uranyl ion adsorption from aqueous solutions. Carbohydr. Polym. **vol. 87**, 2012, pp. 1185–1191. https://doi.org/10.1016/j.carbpol.2011.08.095

[15]. *E. Zolfonoun, S.R. Yousefi,* Sorption and preconcentration of uranium and thorium from aqueous solutions using multi-walled carbon nanotubes decorated with magnetic nanoparticles. Radiochim. Acta, **vol. 103**, 2015, pp. 835–841. https://doi.org/10.1515/ract-2015-2466

[16] *I.M. Nafliu, H.N.A. Al-Ani, A.R. Grosu (Miron), P.C. Albu, G. Nechifor,* Iono-molecular separation with composite membranes. VIII. recuperative aluminium ions separation on capilary polypropylene S-EPDM composite membranes. Mat. Plast. **vol. 56**, no. 1, 2019, pp. 32-36 https://doi.org/10.37358/mp.18.4.5064

[17]. A. Khaliq; M.A. Rhamdhani; G. Brooks; S. Masood; Metal Extraction Processes for Electronic Waste and Existing Industrial Routes: A Review and Australian Perspective. Resources **2014**, *3*, 152-179. https://doi.org/10.3390/resources3010152

[18]. V. Rai; D. Liu; D. Xia; Y. Jayaraman, J.-C.P. Gabriel; Electrochemical Approaches for the Recovery of Metals from Electronic Waste: A Critical Review. Recycling **2021**, *6*, p. 53. https://doi.org/10.3390/recycling6030053

[19]. Y. Zhao; O. Pohl; A.I. Bhatt; G.E. Collis; P.J. Mahon; T. Rüther; A.F. Hollenkamp; A Review on Battery Market Trends, Second-Life Reuse, and Recycling. Sustain. Chem. **2021**, *2*, pp. 167-205. https://doi.org/10.3390/suschem2010011

[20]. *Xue, Y.; Fu, R.; Xu, T.* (-03). Preparation of speek and speek/chitosan composite proton-exchange membranes for application in direct methanol fuel cells. Acta Polymerica Sinica, vol. **03**, 2010, pp. 285-291.

[21]. *A.C. Nechifor, A. Goran, V.-A. Grosu, C. Bungău, P.C. Albu, A.R. Grosu, O. Oprea, F.M. Păncescu, G. Nechifor*, Improving the Performance of Composite Hollow Fiber Membranes with Magnetic Field Generated Convection Application on pH Correction. Membranes, **vol. 11**, 2021, p. 445. https://doi.org/10.3390/membranes11060445

[22]. *A.M. Cimbru, A.A.K.K. Rikabi, O. Oprea, A.R. Grosu, S.-K. Tanczos, M.C. Simonescu, D. Pașcu, V.-A. Grosu, F. Dumitru, G. Nechifor*, *pH* and *pCl* Operational Parameters in Some Metallic Ions Separation with Composite Chitosan/Sulfonated Polyether Ether Ketone/Polypropylene Hollow Fibers Membranes. *Membranes*, **vol. 12**, 2022, p. 833. https://doi.org/10.3390/membranes12090833

[23]. *A.C. Nechifor, A. Pîrțac, P.C. Albu, A.R. Grosu, F. Dumitru, I.A; Dimulescu (Nica), O. Oprea, D. Pașcu, G. Nechifor, S.G. Bungău,* Recuperative Amino Acids Separation through Cellulose Derivative Membranes with Microporous Polypropylene Fiber Matrix. Membranes, **vol. 11**, 2021, p. 429. doi: 10.3390/membranes11060429

[24]. *M. Rožmarić, A.G. Ivšić, Ž Grahek,* Determination of uranium and thorium in complex samples using chromatographic separation, ICP-MS and spectrophotometric detection. Talanta, **vol. 80**(1), 2009, pp. 352–362. https://doi.org/10.1016/j.talanta.2009.06.078.

[25]. *A.G. Fogg, D.R. Marriott, D.T. Burns*, The spectrophotometric determination of tungsten with thiocyanate. Part I. A review of procedures. Analyst, **vol. 95**(1135), 1970, pp.848-853.

[26]. *M. Ghimpusan, G. Nechifor, A.C. Nechifor, S.O. Dima, P. Passeri*, Case studies on the physical-chemical parameters' variation during three different purification approaches destined to treat wastewaters from food industry. J. Environ. Manag. **vol. 203**, 2017, pp. 811–816, doi:10.1016/j.jenvman.2016.07.030.

[27]. *P. Prioteasa, V. Marinescu, A. Bara, M. Iordoc, A. Teisanu, C. Banciu, V. Meltzer*, Electrodeposition of Polypyrrole on Carbon Nanotubes/Si in the Presence of Fe Catalyst for Application in Supercapacitors. Rev. Chim. **vol. 66**, 2015, pp. 820-824

[28]. *L.-G. Zamfir, L. Rotariu, V.E. Marinescu, X.T. Simelane, P.G.L. Baker, E.I. Iwuoha, C. Bala*, Non-enzymatic polyamic acid sensors for hydrogen peroxide detection. Sensors and Actuators B: Chemical, **vol. 226**, 2016, *pp.* 525-533. https://doi.org/10.1016/j.snb.2015.12.026

[29]. *K.N. Han*, Characteristics of Precipitation of Rare Earth Elements with Various Precipitants. Minerals **vol. 10,** 2020, p. 178. https://doi.org/10.3390/min10020178

[30]. *M.I.; Nave, K.G. Kornev*, Complexity of Products of Tungsten Corrosion: Comparison of the 3D Pourbaix Diagrams with the Experimental Data. Metall. Mater. Trans. A, **vol. 48,** 2017, pp.1414–1424. https://doi.org/10.1007/s11661-016-3888-6

[31]. *A.R. Grosu, I.M. Nafliu, I.S. Din, A.M. Cimbru, G. Nechifor*, Neutralization with simultaneous separation of aluminum and copper ions from condensed water through capillary polypropylene and cellulose. UPB Sci. Bull. Ser. B Chem. Mater. Sci. **vol. 82**, 2020, pp. 25–34

[32]. *F.M. Păncescu, A. Ferencz (Dinu), V.A. Grosu, A Goran, Gheorghe Nechifor,* U.P.B. Sci. Bull., Series *B* 2023, 85 (1), pp.77-88

[33]. *A.C. Nechifor, S. Cotorcea, C. Bungău, P.C. Albu, D. Pașcu, O. Oprea, A.R. Grosu, A. Pîrțac, G. Nechifor,* Removing of the Sulfur Compounds by Impregnated Polypropylene Fibers with Silver Nanoparticles-Cellulose Derivatives for Air Odor Correction. Membranes **vol. 11**, 2021, p. 256. https://doi.org/10.3390/membranes11040256

[34] *G.T. Man, P.C. Albu, A.C. Nechifor, A.R. Grosu, D.I. Popescu (Stegarus), V. Grosu, V.E. Marinescu, G. Nechifor*, Simultaneously Recovery of Thorium and Tungsten by Hybrid Electrolysis–Nanofiltration Processes. *Preprints* **2023**, 2023121375. https://doi.org/10.20944/preprints202312.1375.v1